Title

Adaptation of the Generalized Carnot Cycle to Describe Thermodynamics of Cerebral Cortex

Journal

IEEE Press, 1(1)

Author

Freeman, Walter J, III

Publication Date

2012-06-10

Adaptation of the Generalized Carnot Cycle to Describe Thermodynamics of Cerebral Cortex

Freeman WJ, Kozma R, Vitiello G (2012) Adaptation of the generalized Carnot cycle to describe thermodynamics of cerebral cortex. Proc IEEE World Congr Comp Intell WCCI/IJCNN 2012 Brisbane QLD. Australia 10-15 June 2012 IEEE Press, pp. 3229-3236.

Walter J Freeman
Dept of Molecular &Cell Biology
University of California
Berkeley CA 94720 USA

Robert Kozma
Dept of Mathematics
Memphis University
Memphis TN 38152 USA

Giuseppe Vitiello
Facolta di Scienze and Istituto Nazionale
di Fisica Nucleare Università di Salerno
I-84100 Fisciano (Salerno), Italy

Abstract—**The brain is a thermodynamic system operating far from equilibrium. Its function is to extract microscopic sensory information from the volleys of action potentials (pulses) that are delivered by immense arrays of sensory receptors, construct the macroscopic meaning of the information, and store, retrieve, and update that meaning by incorporating it into its knowledge base. The function is executed repetitively in the action-perception-assimilation cycle. Each cycle commences by a phase transition, in which the immense population comprising each sensory cortex condenses from a gas-like state to a liquid-like state. It ends with return of the cortex to the expectant gas-like state. We have modeled the microscopic thermodynamics of the cycle using quantum field theory. Our new result is modeling cortical macroscopic thermodynamics with the generalized Carnot cycle, in which the energy required for the construction of knowledge is supplied by brain metabolism and is dissipated as heat by the cerebral circulation. What makes the application possible is the unprecedented precision with which spatial patterns of ECoG are measured, thus providing precise state variables with which to represent energy vs. entropy. We present experimental evidence that these isothermal processes are coupled by adiabatic cooling and heating. We postulate that the action-perception-assimilation cycle comprises minimally three consecutive Carnot cycles required for basic perception, assimilation, and decision, and more cycles with greater complexity of cognitive tasks at hand.**

Keywords-: action-perception cycle; Carnot cycle; dissipation; electrocorticogram; entropy; Hebbian assembly; non-equilibrium thermodynamics; oxygen debt; phase transition; reinforcement learning; self-organized criticality

I. INTRODUCTION

Brains are adept in detecting minute but highly significant pattern fragments embedded in rich and varied contexts. We propose a dynamical model for the perceptual process [1], which is based on studies of brains as thermodynamic systems that operate far from equilibrium and dissipate metabolic energy as heat [2]. Brains create knowledge through reinforcement learning of conditioned stimuli (CS) and store it in the form of landscapes of basins and their attractors [3]. Brains do this by forming Hebbian nerve cell assemblies in cortex by increasing the synaptic connection strength between co-excited neurons over repeated trials.

Each assembly categorizes each presentation of a CS by generalization over equivalent receptors [4]. The entire assembly is ignited by sensory stimulation of any of its members, so it can direct the cortex to the basin of an attractor. Retrieval by the attractor of the fragment of stored knowledge about that CS is done by a phase transition from a background receiving phase of cortex to an active transmitting phase [5]. The requisite transition energy is provided by the ignition of the Hebbian nerve cell assembly, which requires the delivery to the sensory cortex of a CS that is recognized on the basis of prior learning.

The pre-stimulus background cortical activity resembles Rayleigh noise [6]. It contains non-periodic null spikes at which analytic amplitude nears zero. Phase transitions in perception begin at the null spikes [4], because the drop in background activity in the pass band of a preceding burst of oscillation destabilizes the cortex at the null spikes [7]. The sign of the real part of the exponential envelope of the cortical impulse responses reverses from negative to positive, causing cortex to converge to a singularity [7]. That enables capture of cortex by even a very weak stimulus, when it ignites a Hebbian assembly that selects an appropriate basin of attraction. Previously we modeled this operation at the microscopic level in terms of quantum field theory using the time-dependent Ginzburg-Landau equation [1]. Here we address the macroscopic level, using non-equilibrium thermodynamics. We adapt the concepts of spontaneous symmetry breaking (SBS) and the emergence of unitarily inequivalent ground states [8, 9] to phase transitions in water. The output of cortical activity patterns constitutes the mobilization of knowledge. Patterns are newly constructed and broadcast repeatedly at theta rates from the cortical memory.

This work is supported in part by Defense Advanced Research Projects Agency (DARPA) Physical Intelligence Program in an HRL subcontract.

II. Choosing the State Variables for the Thermodynamic Cycle

There is no question that brains are open thermodynamic systems operating far from equilibrium. They do the work of constructing and storing knowledge by burning glucose to make glycogen and adenosinetriphosphate (ATP). Most of the energy is stored in transmembrane ionic concentration gradients. They dissipate free energy in driving ionic currents that generate the electric and magnetic fields, which mediate the action-perception cycle. We detect them with the electrocorticogram (ECoG, Figure 1). We can measure calories in and out as chemical energy and heat, but we cannot now estimate the energy needed for neural pattern formation or pinpoint the amounts of energy actually used in performing the tasks. As a first attempt to grasp the problem we adapt the Carnot cycle as a framework in which to describe the thermodynamics of perception. The Carnot cycle is an idealized heat engine with four stages. In a steam engine heat is used to do work in one stage and dissipated in another stage. In a refrigerator the work is done followed by heat dissipation. The two ideal stages are isothermal (fixed temperature despite heat exchanges). They are coupled through two other stages: adiabatic compression and expansion (changes in temperature with none in heat content).

We find it convenient to replace the pressure-volume diagram with a temperature-entropy diagram, in which we use two time-varying scalar variables that we can calculate from measurements of multichannel 8x8 ECoG recordings (Figure 1). Corresponding to pressure and temperature we use scalar mean power, $\underline{A}^2(t)$, the square of the analytic amplitude of the time-dependent vector specifying the rates of energy dissipation at the multiple sites of recording. Corresponding to volume and entropy is our order parameter, which we represent by the normalized (n x 1) feature vector specifying the spatial pattern of amplitude modulation of a carrier frequency. The vectorial order parameter designates a point in n-space (n = 64 electrodes in an 8 x 8 array, Figure 2), designating an AM pattern which is constructed by cortical dynamics.

The feature (n x 1) vector serves to classify bursts of oscillation with respect to behavior by clusters of points in n-space [3] but not for graphic display of the thermodynamic cycle, so we represent it with a scalar index: the rate of change in the spatial pattern of amplitude modulation (AM), which we measure by calculating changes in Euclidean distance, $\Delta D_e(t)$, between successive points, $D_e(t)$, in n-space for each beta or gamma carrier wave [10, 11]. Low values reflect the degree of order that is imposed to form, hold and transmit the AM pattern. High values reflect disorder (high entropy).

III. The Neurobiological Burst of Oscillation

The main work of cortex is done by the dendrites, which generate the electric synaptic currents that control the pulse density in each local area. The currents in the cortex also sustain fields of dendritic potential (the electrocorticogram, ECoG, Figure 1). The alignment of the cortical neurons in palisades and layers facilitates summation of the synchronized dendritic potentials of the interactive neurons, giving the mesoscopic state variable, $V_{x,y}(t)$, that represents the ECoG amplitude at each time point and cortical location, x,y. When subjects are at rest, the activity is unstructured with 1/f spectra (Figure 3, A). Because of the lack of classifiable AM patterns, we infer resting is the equivalent of a symmetric vacuum state in which no work is being done (Figure 1, B). Upon arousal (Figure 1, A) the ECoG reveals AM patterns in bursts formed by spontaneous breaking of symmetry (SBS). Between bursts the cortex returns to the unpatterned background activity, which manifests a domain of self-organized criticality (SOC) [12], in which the cortex holds itself near threshold for a phase transition by myriad 'neural avalanches' having scale-free distributions of frequency and duration [13] that dissipate the energy released by random background pulse input.

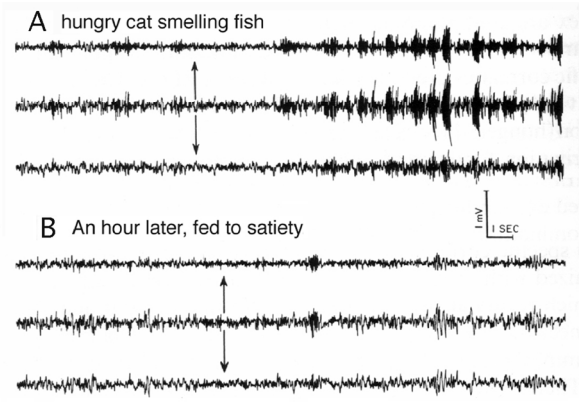

Figure 1. ECoG recordings from olfactory cortex. **Above.** A food-deprived cat at rest is aroused by an odor of fish and searches for it by sniffing. **Below.** After feeding to satiety there is no arousal. The upper and lower signals were recorded from the surface and depth of the olfactory cortex; the middle signal is the difference across the dipole field of the cortical pyramidal cells. (From Fig. 7.17 p. 442 in [7]).

When subjects are aroused (Figure 1, A), bursts of narrow band oscillation emerge, reflecting increases in both pulse density and pulse coherence that manifest intermittent increases in use and dissipation of free energy. The ECoG measured with an 8x8 array of electrodes reveals a spatial pattern of amplitude modulation (AM) of the carrier wave of each burst (Figure 2). The spatial AM patterns reflect the perception of familiar sensory stimuli (CS) given to subjects. They reveal the order that the subjects create from chaotic background oscillations, using the energy stored in transmembrane ionic gradients.

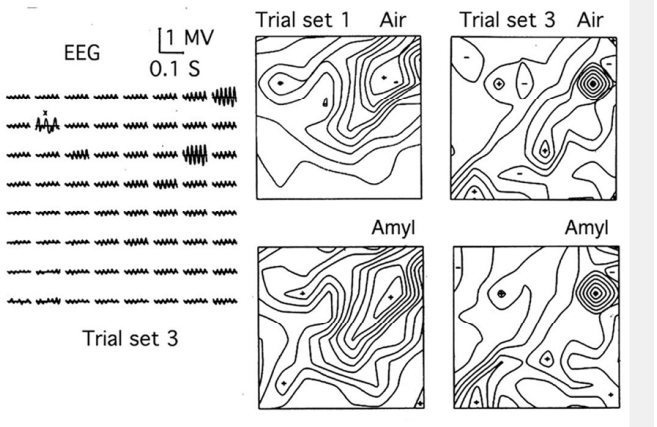

Figure 2. Spatial patterns of wave packets in ECoG. **Left:** Example of AM carrier wave in one frame. **Right:** Contour plots of AM patterns from 8x8

electrodes (3.5x3.5 mm) in frames showing differences that were correlated with conditioned stimuli (CS) by means of pattern classification [3].

Power spectral density (PSD) calculated long term (>1 s) gives 1/f relations of log power to log frequency. Short term (<100 ms) gives multiple peaks with narrow pass bands (Figure 3, A). Band pass filtering encompassing the peaks in the short term PSD reveals the beats corresponding to the bursts that are triggered by conditioned stimuli (Figure 3, B). Usually there are multiple overlapping frequencies of oscillation as shown in Figure 3, B, only one of which may be correlated with the CS.

The frequency modulation observed from each burst to the next enjoins use of the Hilbert transform [14]. The optimal spatiotemporal resolution of the activity density for pattern classification is given by the analytic power of the signal at each electrode, $A_{x,y}^2(t)$, which is the square of the analytic amplitude from the Hilbert transform (Figure 3, C) of each band pass filtered ECoG signal, $V_{x,y}(t)$ [11].

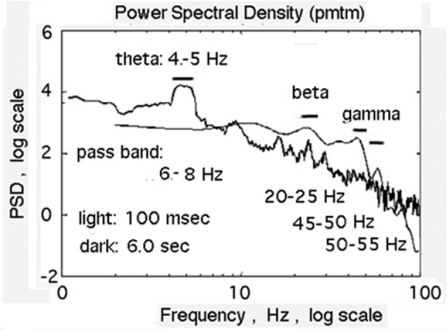

Figure 3, A. Short-term power spectral density (PSD) reveals multiple overlapping components with differing center frequencies and pass bandwidths.

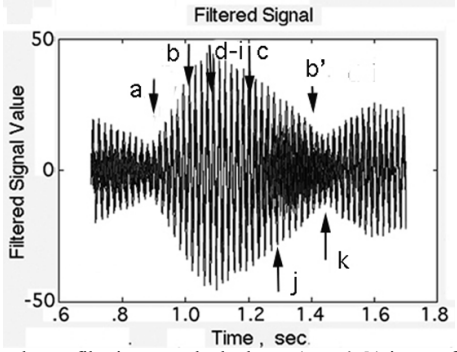

Figure 3, B. Band pass filtering reveals the beats (**a, c, j, k**) in two frequencies in $V_{x,y}(t)$ due to band pass filtering. Beat intervals are set by pass bandwidth [6]. Onset of one is at c, offset at k; onset of the other is at c, offset at k. The scale is in microvolts.

Thereby the AM pattern of the ECoG gives us the vectorial order parameter in a matrix, $\mathbf{A}^2(t)$, which indirectly reveals the intensity of synaptic interactions at high feedback gain among a population of neurons constructing a percept [7]. For purposes of graphic display our scalar index of power shown by the ECoG is the $\log_{10}$ mean power, $\underline{A}^2(t)$, derived from 64 signals (Figure 3, C) at each time step. The analytic phase, $\phi(t)$, after unwrapping is measured with respect to phase at an arbitrary starting point. The analytic frequency, $\omega(t)$, is calculated in rad/sec by dividing the difference between successive phase values by the duration of the digitizing interval, Δt (Figure 3, D). Bursts usually began with a discontinuity in $\phi(t)$ [11].

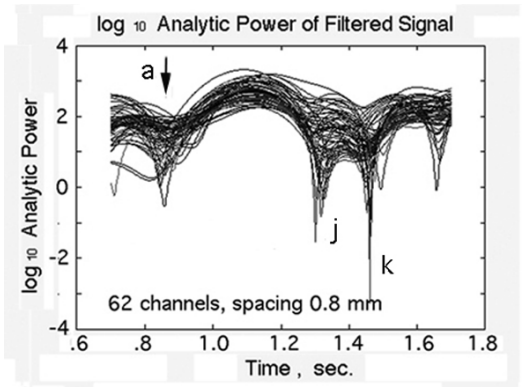

Figure 3, C. Log_{10} analytic power feature vector of an AM pattern (**a-k**). The signals from two bad channels were deleted.

Division by 2π gives the frequency in Hz. The minimal spatial $SD_X(t)$ of the 64 values of $\omega(t)$ in the interval between beats (d-i) serves to evaluate the width of the pass band of the carrier frequency [4]. The width of the pass band determines the interval between successive beats [6].

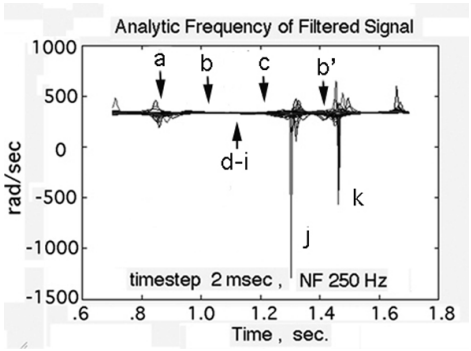

Figure 3, D. The analytic frequency, $\omega(t)$, shows high coherence (**d-i**).

IV. The Classic Carnot Cycle

An example of a sequence of bursts is shown in Figure 4 after filtering in the high beta range. There is a dominant stationary frequency band in each burst, which is most likely to have an AM pattern. Frame A shows 1 s recording of 64 superimposed ECoG signals filtered in the pass band 20-28 Hz. Frame B shows the 64 time series of analytic power. Frame C shows $\log_{10}$ analytic power. Frame D shows the 64 time series of the analytic frequency, $\omega(t)$. The arrows indicate the minimum in each frame of the $SD_X(t)$ of the 64 frequencies, which we used to evaluate the pass bandwidth of the carrier frequency [4].

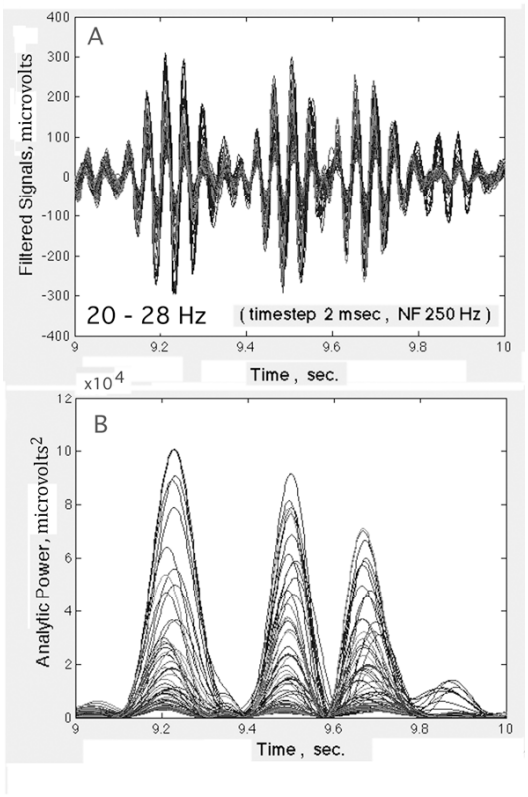

Figure 4. A.B. Decomposition of 64 ECoG signals with the Hilbert Transform.

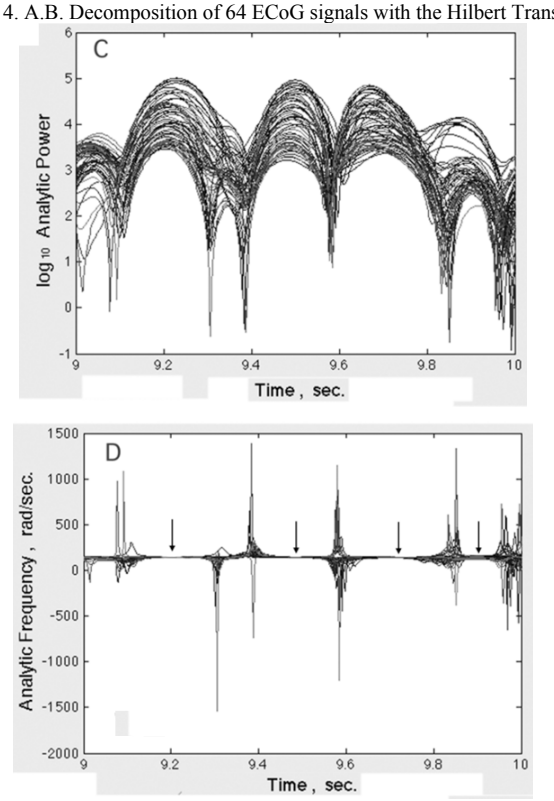

Figure 4, C, D. Decomposition of 64 ECoG signals with the Hilbert Transform. Log_{10} analytic power © reveals null spikes that we use as markers for frame onsets. The mean at the arrows gives the carrier frequency, The minima in $SD_X(t)$ (arrows) give the width of the carrier pass band [4].

We adapt the Carnot formalism to cortex by conforming to the four processes that comprise the ideal Carnot cycle, which is illustrated in a temperature-entropy diagram (Figure 5). We start our cycle at minimal temperature and maximal disorder (1). Free energy is dissipated as matter compresses into a highly ordered state (A), which decreases the entropy [15] without increasing the temperature or pressure (2). The temperature increases by adiabatic compression (B) to maximal power without change in order (3). Upon introduction of energy as heat the matter undergoes isothermal expansion (C) to a disordered state (4), and it returns to its initial state (1) by cooling with adiabatic expansion without further change in energy (D).

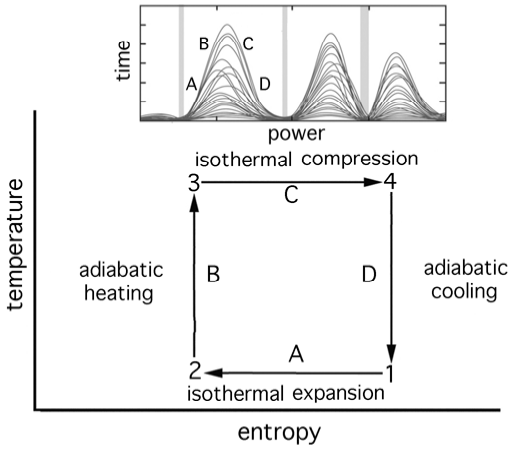

Figure 5. The classic Carnot cycle for fluid is shown as temperature vs. entropy.

On translating the properties of the cycle into neural terms, we conceive the cycle as beginning with the minimum of $A^2(t)$, at which pre-existing structure is expunged from the cortical dynamics on returning to the background state of symmetry (1). Burst onset is manifested in a null spike (Figure 4, C). In this stage (1-2 in Figure 6) the pulse density of activity is sustained by input of pulses from many sources in the brain (denoted by neurobiologists as *centrifugal*) and from sensory receptors. If the input contains pulses from a CS, the pulses ignite a Hebbian assembly formed by prior learning. The local high density of firing in the assembly triggers a global change in activity, which is not expressed by an increase in the number of pulses per unit volume but by an increase in the coherence of neural firing at the carrier frequency, which increases $A^2(t)$. This means that the released energy is not distributed among the system degrees of freedom in the form of thermalizing kinetic energy [1]. Instead it is used to promote the collective long-range correlation modes among the interacting neurons. Each cortical neuron connects with 10^4 others, then 10^8, 10^{12}, and so on, leading in very few serial synaptic steps to the condensed state (2), in which every neuron contributes directly to cortical output, whether its firing rate is low or high. It is the recruitment of all neurons into the dense phase that provides the richness of context required to express knowledge.

We conceive that the dense phase is the prerequisite for the expression of knowledge about a stimulus at immediate expense of the potential energy in ionic gradients that is converted to kinetic energy of ionic flows and then to heat, which is removed by the circulation. The energy mobilizes an attractor landscape, ignites a Hebbian assembly, guides the cortex into one of the basins of attraction, and organizes the spatial AM pattern of the

carrier wave. Energy expenditure continues in stage (2-3) (Figure 6), with increases in pulse density as revealed by further increase in $\underline{A}^2(t)$ to (3). We conceive that the main work of constructing knowledge is done in stage (1-2), when the AM pattern forms, and the cortex exits the basin of a non-zero point attractor that governs the background activity [7, 16] and converges to a limit cycle attractor that governs the burst [17]. The compression expresses the strength of synaptic interaction from having a feedback gain that exceeds unity [15]. Amplification and transmission of selected AM patterns occur at high pulse density in stage (2-3).

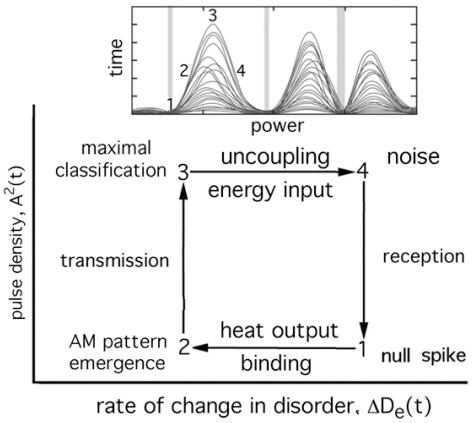

Figure 6. The coordinates are expressed in terms of two variables that can be measured using the ECoG replacing temperature or pressure by pulse density (measured by $A^2(t)$) and entropy by volume or coherence (measured by the rate of change in spatial AM pattern of the feature vector, $\Delta D_e(t)$).

All these processes dissipate substantial metabolic free energy and incur what biologists refer to as an oxygen debt, meaning an expenditure of free energy that must be repaid by oxidative metabolism. In other words, neurons immediately converge to an attractor by dissipating free energy (cooling, condensing) and later replenish it by burning glucose to make ATP and restore the transmembrane ionic gradients.

The density of phase-locked, spatially coherent pulses contributes to $A^2(t)$ in two ways: the number of pulses per unit volume, and the degree of synchrony in firing. Both tend to fluctuate together. In our idealized first approximation we define the temperature in neural terms as the pulse density per unit volume (space) and the pulse density per unit time as the degree of coherence and inversely to the degree of disorder, entropy. An empirical measure of the degree of order is provided by the rate of change in the nx1 feature vector that defines AM patterns. This variable is the rate of change in the Euclidean distance, $\Delta D_e(t)$, between each pair of successive points in n-space [11, 18]. When the step size is small, we infer from the relative stationarity of the AM pattern that the degree of order is high. Both $A^2(t)$ and $D_e(t)$ are derived from the ECoG. They differ in that $A^2(t)$ is the spatial mean of the analytic power at each step, while $D_e(t)$ is the step-wise temporal difference of the feature vector after normalization of each frame (subtracting the frame mean and dividing by the spatial standard deviation). One indexes the rate of consumption of free energy, and the other indexes the rate of decrease in order (increase in entropy).

From stage (2) the rise in $\underline{A}^2(t)$ continues to stage (2-3) (B in Figure 5), owing to an increase pulse density to peak values that are commonly seen in transient bursts of pulse activity at the microscopic level. The synaptic interaction carries the cortical populations to a peak in wave power, $\underline{A}^2(t)$ (3), all the while transmitting the AM pattern. We regard the transmission (B in Figure 5) as a form of adiabatic heating with further depletion of potential energy and increase in the oxygen debt, but with no further increase in order.

The decline in $\underline{A}^2(t)$ from the peak value (3) in stage C is by reduction in both pulse density and pulse coherence with return to microscopic sparse coding. The extreme density diminishes along with the strength of synaptic interaction, leading to a phase transition with no discontinuity in the analytic phase, $\phi(t)$ [1, 15]. The energy expended in generating coherence and order in the neural activity is repaid. The payment of the oxygen debt is revealed by BOLD (blood oxygen level depletion) and fMRI (functional magnetic resonance imaging) [19, 20]. We conceive that the reduction in $A^2(t)$ manifests uncoupling as a passive process from (3-4) that requires no metabolic energy. The payment of the oxygen debt to replenish the energy store is done at rates up to 2 or 3 orders of magnitude slower. A similar mechanism of "act now, pay later" is well known in muscle, in which the expenditure of metabolic energy by breakdown of ATP is required during muscle relaxation, not contraction.

Stage (4-1) is reduction in density corresponding to adiabatic cooling. This was demonstrated at the single neuron level in a little known but remarkable tour de force, in which Bernard Abbot demonstrated cooling of an axon upon the expansion of sodium ions into the interior with each action potential [21]. As the neurons uncouple, they become again receptive to input from sensory receptors ("reception"). We attribute the continuing decline in $A^2(t)$ to the statistical properties of the background activity of cortex [4] as modeled by the Rice distribution of extreme values [6], giving rise to the beats seen in Rayleigh noise (Figure 3). The beat frequency is determined by the width of the pass band around the center frequency of each beta or gamma burst elicited by input (Figure 1). The distribution of times of onset of the null spike initiating the next phase transition is predicted by Rice statistics. The uncertainty imposed by the unpredictability of onset latency shows that the symmetry breaking is spontaneous. Hence we infer that stage D is passive adiabatic cooling not involving a change in energy. It is the release of cortical neurons from the tight binding in the condensed state that allows them to respond to sensory and centrifugal inputs [15].

V. The Generalized Carnot Cycle

We again adapt the four stages around the cycle, this time addressing some properties introduced by phase transitions (Figure 7). We use the phase portrait that portrays the phase space for mixtures of gas and liquid water such as vapor [22], in which a steady state prevails in a domain of criticality [1, 15]. In doing so we begin at stage (1), the minimum of pressure (sparseness of pulse density) and maximum volume (maximum disorder, entropy). In water the temperature and pressure are almost constant during condensation afforded by an outflow of energy as heat, Q_C (1-2). An adiabatic increase in pressure results from energy used to compress the mixture (2-3), which carries the mixture to maximum power and order (minimal

volume). Upon evaporation (3-4) energy input is required, Q_H. In the last step an adiabatic decrease in pressure results in cooling (4-1) (no change in pattern despite decrease in power).

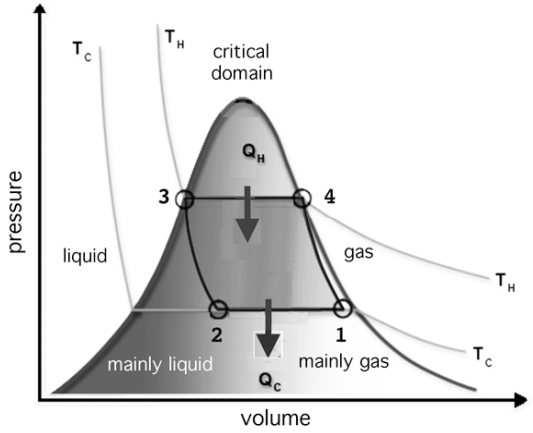

Figure 7. The four segments that comprise the generalized Carnot cycle are shown embedded in a domain of criticality, in which the gas and liquid phases coexist in varying degree. We conceive the operation of cortex as taking information from stage 1 and constructing and transmitting knowledge by stage 3. Energy flows in as metabolic chemical energy, Q_H, and flows out as heat, Q_C. Adapted from [22]

In stage (1) we conceive the cortical population as existing mainly in a gas-like phase of maximal disorder with aperiodic firing and minimal coherence. We attribute the initial rise in power, $\underline{A}^2(t)$ (A in Figure 6) to cortical neurons released from prior binding and firing in response to a broad range of centrifugal and sensory input. If the sensory input carries information in a CS, the ignition of a Hebbian assembly facilitates the formation of an intense burst of narrow band oscillation, which sets the stage for selection of a basin of attraction (1-2). During this early increase in $\underline{A}^2(t)$ the AM pattern emerges (2), and the accompanying spatial pattern of phase, $\phi(t)$, is laid down. The emergence of the AM pattern selected by the Hebbian assembly precipitates spontaneous breaking of symmetry [9].

In this stage the energy given to the system by diminution of ionic gradients is not in the form of kinetic energy distributed among the neurons, but it is given to collective modes responsible for the long-range coherent oscillations among the neurons. Entropy is accordingly decreasing, since order is thereby constructed. In the field model this is depicted as the isothermal increase in the runaway excitation of neurons leading to the coherence of firing in the condensed ground phase (cf. Eqs. B.7, 9 and 33 in [8], [9] and [1] respectively). The onset is marked by a discontinuity in the analytic phase, $\phi(t)$ [4]. The sequestration of energy in the coherence also corresponds to the lower energy state into which the cortex is 'attracted'.

The gate for further input to cortex is shut. The receiving phase ends, and the transmitting stage (B) begins. Mutual excitation in positive feedback at greater than unity gain increases the rates of firing with no further increase in coherence or reduction in entropy. The increase in firing rate with runaway excitation manifests an increase in temperature and further increase in oxygen debt. In stage (C) $A^2(t)$ falls as the refractory periods of the neurons saturate the firing rates, and the neurons uncouple as by evaporation. At this stage the repayment is begun of the energy deficit carried, initially by depletion of energy stores in ATP and glycogen, and more slowly by oxidative metabolism. In the final stage (D) the interference from Rayleigh noise causes $A^2(t)$ to fall to near zero in null spikes, manifesting maximal disorder and entropy but without further decrease in energy dissipation, which we treat as adiabatic cooling,.

VI. Conclusions

The value of the Carnot formalism in the 19th century was the clarification it brought to solving the problems of developing efficient steam engines, which required advances in technology but equally in the emergence of a new branch of physics. It served as a crystal from which grew the concept of entropy and the first and second laws of thermodynamics. In the present century it may again serve to bring in to focus a core concept, which is to understand how cortices so efficiently select and integrate fragments of information acquired through experience, store it as knowledge, and deploy that knowledge in the action-perception-assimilation cycle. We emphasize that the Carnot formalism requires varying each state variable in turn while fixing all others. By virtue of that separation of variables the formalism enables us to bring into focus the several disciplines of EEG and ECoG research [11], neuropsychology [3, 23], brain imaging as measured by fMRI [19, 20], computational models of information processing in intentional robotics [24], neuropercolation in random graph theory [25], and quantum field theory [1, 2]. The Carnot formalism is consistent with models that define 'free energy' as uncertainty [26] yet avoids the difficulties incurred in applying Shannonian theory to semantics when attempting to measure knowledge.

We emphasize that our application of the Carnot formalism to non-equilibrium thermodynamic brain processes requires us to define state variables that serve as representations for the rates of change in energy and entropy in each segment of the cycle. We have derived variables that we have calculated from measurements of multidimensional neural activity patterns with unprecedented precision in time, space and frequency. In other words, the physics is 200 years old; the techniques for making estimates of the work done by the brain to create knowledge are very new. Moreover, the cycle is not a closed loop. It is the projection into a plane of a helix in time, which allows for the continual incremental growth of knowledge in the brain.

On the one hand the ideal Carnot cycle (Figure 5) treats cerebral cortex as metastable [27], as it shifts across a continuum between sparse activity at low density and intense activity at high density. On the other hand, the generalized Carnot cycle (Figure 7) treats cortex as bistable [28], because there is a qualitative difference between an evaporated phase and a condensed phase. Condensation by phase transition requires an irreversible convergence to an attractor, which expresses a collective mode that has been modeled at the microscopic level using the time-dependent Ginzburg-Landau equation [1]. This success opens the way to explication of the transition at the macroscopic population level in terms of thermodynamics, for which preliminary approaches using classical equilibrium [29, 30] and pseudo-equilibrium thermodynamics [15] have already been undertaken.

An issue that we leave unresolved is whether in the transition (1-2) from the sparse mode to the high-density mode there is any form of energy taken up that is equivalent to the latent heat of vaporization of water, which is released as heat (3-4). We cannot resolve the issue experimentally until we have devised better methods for distinguishing and measuring changes in pulse density due to firing rates or to firing coherence, and until we have devised tools for measuring the local fluctuations in cortical temperature that we predict will be found in association with AM pattern formation [1].

The importance of thermodynamics for brain science is underscored by the fact that brains dissipate free energy at rates ten times greater than any other organ, at rest in maintenance and repair, and at work in all types of intentional planning, predicting and acting. The all-inclusive, macroscopic method is to measure BOLD and fMRI [19, 20]. What is needed is a scale-free formalism that can apply both at the microscopic cellular level [1] and at the mesoscopic population level [15], as well as the macroscopic behavioral level [23]. We believe that the Carnot formalism might catalyze recognition of the existence of a liquid-like phase of cortical neuropil and the phase transitions by which cortex enters from and returns to a gas-like phase.

In its present form the Carnot formalism has been adapted to the mesoscopic level at which the cortex uses the sensory information delivered by conditioned stimuli (CS) to select a percept and transmit it as an AM pattern. Looking upwardly we propose that this same neural mechanism repeats at the macroscopic level, when the percepts from all of the sensory cortices combine in the limbic system into concepts and gestalts, and then in the motor cortices during the selection and implementation of intentional action. We cite evidence that the same mechanism holds in higher cognitive functions that require coherence of neural oscillations over the entire brain [31-33]. Looking downwardly we see the possibility of applying the same Carnot formalism through the mesoscopic Hebbian assemblies to the microscopic assemblies of water molecules in solutions, through which ions move in electric currents that execute the basic neural functions of integration and transmission [1]. This clarification may be necessary to define the state variables needed to draw a phase diagram for cortex resembling but differing from that for water (Figure 7).

The Carnot formalism fits only qualitatively to our ECoG data. On the experimental side this is mainly because the data were not collected with the overt aim of testing thermodynamic models, and because the spatial, temporal and spectral resolutions that were available at the time of collection were not fully adequate to resolve the fluctuations in power, phase, and frequency that will be required to thoroughly test new hypotheses. On the theoretical side a key unsolved problem is posed by the fact that changes in power, $A^2(t)$, occur by changes in the number of neurons contributing and by the degree of synchronization of their pulse probabilities. Development of theory is needed to define new state variables that, on the one hand, adequately represent temperature and entropy and, on the other hand, can be evaluated unequivocally by calculations from experimental data. Theory may be crucial also in the design of new experimental techniques needed to measure local fluctuations in temperature [21, 31] and in multiunit recording of action potentials in order to estimate pulse density directly instead of by inference from the ECoG. We think that the greatest challenge we face is in the development of new signal processing procedures [18, 321] with which to decompose and measure the individual bursts that overlap in the raw ECoG (cf. Figure 3, B).

We speculate that this non-equilibrium thermodynamic cycle emerged in the evolution of reptilian brains to service olfactory perception, and that it was adapted thereafter in all sensory systems on emergence in mammals of neocortex and then as a key mechanism for gestalt and concept formation in the limbic system. Because of its scale-free dynamics it was extended to levels of higher cognition that encompass vast areas of the cerebral cortex in the construction and activation of knowledge [31-32].

Today as in the 19th century the stakes are very high for the development of brain theory that suffices to meet the needs for applications in new forms of machine intelligence and brain-machine interfacing. An initiative that is very bold indeed is required to link knowledge to the firing of neurons in a system that knows what it is doing, whether it is biological or artificial.

REFERENCES

[1] Freeman WJ, Livi R, Obinata M, Vitiello G (in press) Cortical phase transitions, non-equilibrium thermodynamics and the time-dependent Ginzburg-Landau equation. Int J Mod Phys B (in press) arxiv:1110.3677v1 [physics.bio-ph]

[2] Vitiello G (2001) My Double Unveiled. Amsterdam: John Benjamins

[3] Freeman WJ. (1999). How brains make up their minds. Weidenfeld & Nicholson, London.

[4] Freeman WJ [2009] Deep analysis of perception through dynamic structures that emerge in cortical activity from self-regulated noise. Cog Neurodyn 3(1): 105-116. http://www.springerlink.com/content/v375t5l4t065m48q/

[5] Kozma R, Puljic M, Balister P, Bollabás B, Freeman WJ. (2005) Phase transitions in the neuropercolation model of neural populations with mixed local and non-local interactions. Biol. Cybern. 92: 367-379. http://repositories.cdlib.org/postprints/999

[6] Rice SO [1950] Mathematical Analysis of Random Noise - and Appendixes – Technical Publications Monograph B-1589. New York: Bell Telephone Labs Inc.

[7] Freeman WJ (1975) Mass action in the nervous system. Examination of the neurophysiological basis of adaptive behavior through the EEG. Academic Press, New York. Posted in e-formats (2004) http://sulcus.berkeley.edu/MANSWWW/MANSWWW.html

[8] Freeman WJ, Vitiello G (2006) Nonlinear brain dynamics as macroscopic manifestation of underlying many-body field dynamics. Phys Life Rev 3: 93-118. http://dx.doi.org/10.1016/j.plrev.2006.02.001

[9] Freeman WJ, Vitiello G (2008) Dissipation and spontaneous symmetry breaking in brain dynamics. J Physics A: Math, Theory 41 – 304042 (17 pp) doi:10.1088/1751-8113/41/30/304042 http://stacks.iop.org/1751-8121/41/304042

[10] Barrie JM, Freeman WJ, Lenhart M (1996) Modulation by discriminative training of spatial patterns of gamma EEG amplitude and phase in neocortex of rabbits. J Neurophysiol 76:520-539

[11] Freeman W.J. [2004] Origin, structure, and role of background EEG activity. Part 1. Analytic amplitude. Clin. Neurophysiol. 115: 2077-2088. http://repositories.cdlib.org/postprints/1006

[12] Plenz D, Thiagaran TC (2007) The organizing principles of neural avalanches: cell assemblies in the cortex. Trends Neurosci. 30: 101-110.

[13] Freeman WJ, Breakspear Scale-free neocortical dynamics. Scholarpedia, 2(2): 1357. http://www.scholarpedia.org/article/Scale-free_neocortical_dynamics

[14] Freeman WJ (2007) The Hilbert transform for EEG. Scholarpedia 2(1): 1338 http://www.scholarpedia.org/article/Hilbert_transform_for brain_waves

[15] Freeman WJ [2008] A pseudo-equilibrium thermodynamic model of information processing in nonlinear brain dynamics. Neural Networks 21: 257-265. http://repositories.cdlib.org/postprints/2781
[16] Freeman WJ, Zhai J (2009) Simulated power spectral density (PSD) of background electrocorticogram (ECoG). Cogn Neurodyn 3(1): 97-103. http://dx.doi.org/10.1007/s11571-008-9064-y
[17] Freeman WJ (1987) Simulation of chaotic EEG patterns with a dynamic model of the olfactory system. Biological Cybernetics 56: 139-150.
[18] Freeman WJ (2011) Understanding perception through neural 'codes'. In: Special Issue on "Grand Challenges in Neuroengineering", IEEE Trans Biomed Engin 58 (7): 1884-1890. DOI: 10.1109/TBME.2010.2095854
[19] Logothetis NK (2008) What we can do and what we cannot do with fMRI. *Nature* 453: 869-878. doi:10.1038/nature06976
[20] Freeman WJ, Ahlfors SM, Menon V (2009) Combining EEG, MEG and fMRI signals to characterize mesoscopic patterns of brain activity related to cognition. Special Issue (Lorig TS, ed.) Intern J Psychophysiol 73(1): 43-52. http://repositories.cdlib.org/postprints/3386
[21] Abbot BC (1960) Heat production in nerve and electric organ. J General Physiol 43: 119-127.
[22] Baratuci Dr. (2011) Learn Thermodynamics http://www.learnthermo.com/T1-tutorial/ch06/lesson-E/pg17.php#
[23] Pribram KH (1991) Brain and perception: Holonomy and structure in figural processing. Mahwah NJ: Lawrence Erlbaum Assoc
[24] Kozma R, Huntsberger T, Aghazarian H, Tunstel E, Ilin R, Freeman WJ (2008) Implementing intentional robotics principles using SSR2K platform. Advanced Robotics 22(12): 1309-1327.
[25] Freeman WJ, Kozma R, Bollobás B, Riordan (2009) Chapter 7. Scale-free cortical planar network, in: Handbook of Large-Scale Random Networks. Series: Bolyai Mathematical Studies, Bollobás B, Kozma R, Miklös D (Eds.), New York: Springer, Vol. 18, pp. 277-324. http://www.springer.com/math/numbers/book/978-3-540-69394-9
[26] Friston K (2009) The free-energy principle: a rough guide to the brain? Trends Cogn Sci **13**(7): 293-301.
[27] Freyer F, Aquino K, Robinson PA, Ritter P, Breakspear M (2009) Bistability and non-gaussian fluctuations in spontaneous cortical activity. J Neurosci 29(26):8512– 8524
[28] Bressler SL, Menon V (2010) Large-scale networks in cognition: emerging methods and principles. Trends Cogn Sci 14: 277-290.
[29] Steyn-Ross ML, Steyn-Ross DA, Sleigh JW, Wilcocks LC (2001) Toward a theory of the general-anesthetic-induced phase transition of the cerebral cortex. I. A thermodynamics analogy. Phys. Rev. E 64, 011917. doi: 10.1103/PhysRevE.64.011917
[30] Wright JJ (2011) Attractor dynamics and thermodynamic analogies in cerebral cortex: synchronous oscillation, the background EEG, and the regulation of attention. Bull Math Biol 73(2): 436-457. doi: 10.1007/s11538-010-9562-zDOI: 10.1007/s11538-010-9562-z
[31] Pockett S, Bold GEJ, Freeman WJ [2009] EEG synchrony during a perceptual-cognitive task: Widespread phase synchrony at all frequencies. Clin Neurophysiol 120: 695-708. doi:10.1016/j.clinph.2008.12.044
[32] Ruiz Y, Pockett S, Freeman WJ, Gonzales E, Li Guang (2010) A method to study global spatial patterns related to sensory perception in scalp EEG. J Neuroscience Methods 191: 110-118. doi:10.1016/j.jneumeth.2010.05.021
[33] Panagiotides H, Freeman WJ, Holmes MD, Pantazis D (2010) Behavioral states may be associated with distinct spatial patterns in electrocorticogram (ECoG). Cogn Neurodyn 5(1): 55-66. doi: 10.1007/s11571-010-9139-4